ELSEVIER

Journal of Molecular Catalysis A: Chemical 179 (2002) 193–200

JOURNAL OF MOLECULAR CATALYSIS A: CHEMICAL

www.elsevier.com/locate/molcata

Photocatalytic activity of hydroxyapatite for methyl mercaptane

Harumitsu Nishikawa [a,*], Koichi Omamiuda [b]

[a] *Gifu Prefectural Institute of Health and Environmental Sciences, 1-1, Naka-fudogaoka, Kakamigahara-shi, Gifu 504-0838, Japan*
[b] *Sumitomo Osaka Cement Co., Ltd., 585, Toyotomi-cho, Funabashi-shi, Chiba 274-8601, Japan*

Received 1 May 2001; accepted 16 August 2001

Abstract

The formation of radical species on stoichiometric hydroxyapatite (HAp) by UV irradiation and the photocatalytic behavior of HAp were studied. The radical species formed on HAp after heat treatment at 200 °C (HAp200) by UV irradiation was assigned to be $O_2^{\bullet -}$ species from the results of electron spin resonance (ESR) studies. Electron transfer must occur from vacancy formed in apatitic structure to oxygen in atmospheric air on HAp. It was recognized that the amounts of $O_2^{\bullet -}$ species on HAp increased by UV irradiation. The conversion of methyl mercaptane (MM) using HAp200 under UV irradiation for 60 min was 96%. That is, the photocatalytic decomposition of MM on HAp200 proceeded effectively. It was suggested that the photocatalytic activity of HAp was due to the production of sufficient amounts of $O_2^{\bullet -}$ species under UV irradiation.

Keywords: Hydroxyapatite; Photocatalysis; Adsorption; Methyl mercaptane

1. Introduction

Hydroxyapatite is commonly used in the fields of bioceramics and absorbent for liquid chromatography. Thermal catalytic character of hydroxyapatite has been reported for the catalytic reaction of alcohol [1,2], cyclohexanon oxime [3] and for the synthesis of phenol [4–6]. We have also reported on the oxidative decomposition of gaseous chlorinated organic compounds over calcium-deficient hydroxyapatite [7–10]. Matsumura et al. [11] have reported oxidation of carbon monoxide over hydroxyapatite.

On the other hand, Kanai et al. [12,13] reported the formation of radical oxygen species on hydroxyapatite and the photo-oxidation of propane and propene over stoichiometric hydroxyapatite (HAp). They concluded that active species were assumed to be labile O^- species by UV irradiation and the species reacted with O_2 to produce O_3^- species from the results of ESR study. In previous studies, the production of O_2^- radical by thermal treatment of HAp was reported [14]. However, the changes of surface state of HAp and the mechanism of radical formation by UV irradiation are not clear. There was also few studies on photocatalytic decomposition mechanism of odor compounds containing sulfur using HAp.

In this paper, we have studied the formation of radical species on the surface of HAp by UV irradiation and photocatalytic behavior of HAp for methyl mercaptane (MM).

2. Experimental

HAp used was prepared from $Ca(OH)_2$ and H_3PO_4 as starting materials [15]. The stoichiometric amounts of H_3PO_4 solution was added dropwise to a $Ca(OH)_2$

* Corresponding author.
E-mail address: p78884@govt.pref.gifu.jp (H. Nishikawa).

1381-1169/02/$ – see front matter
PII: S1381-1169(01)00325-9

slurry. Stoichiometric HAp was prepared by keeping the slurry at pH 7.0 and by aging for 48 h at room temperature. The resulting solid was dried at 100 °C for 24 h. Heat treatment for the solid was carried out at 200 and 1150 °C for 1 h in an electric furnace. Ca/P molar ratio of the solid was 1.67 by chemical analysis.

Fourier transform infrared (FTIR) spectra were measured with a JASCO Hershel FTIR-615 equipped with a microscope M-20 to observe the transmission spectra by the KBr technique. X-ray powder diffraction (XRD) patterns were recorded on a Rigaku Miniflex diffractometer. Electron spin resonance (ESR) spectra were recorded on a JEOL JES-FA200 spectrometer. Radical species were detected as spin adducts [16] and the spin trapping reagent used was 5,5-dimethyl-1-pyrroline-1-oxide (DMPO). ESR spectra of the HAp sample were measured before and immediately after UV irradiation. TG/DTA was measured with a Seiko Instruments Exstar 6000 TG-DTA 6300 using a heating rate of 10 °C/min in a nitrogen stream. BET surface area was measured with a Micromeritics Autopore 9200 at 77 K.

The experimental apparatus for adsorption and photocatalytic reaction for MM is shown in Fig. 1. Adsorption test of MM in air was performed at a flow rate of 70 ml/min in dark condition. Photocatalytic reaction of MM in air was performed at the space velocity of 340 h^{-1}. The light sources used were black-light-type and UV (254 nm)-type (Toshiba Lightec, 8.8 $\mu W/cm^2$ of light intensity). Adsorption or photocatalytic reaction vessel was covered with aluminum foil to shut off the outside light. MM and dimethyl disulfide (DMDS) in inlet and effluent gas were measured by gas chromatograph (Shimadzu GC-15A) equipped with flame photometric detector. SO_2 in effluent gas was measured by a Japan Thermoelectron Model 43C analyzer. Organic acids collected in water at the outlet of the vessel were measured by ion chromatograph (Shimadzu organic acid analysis system).

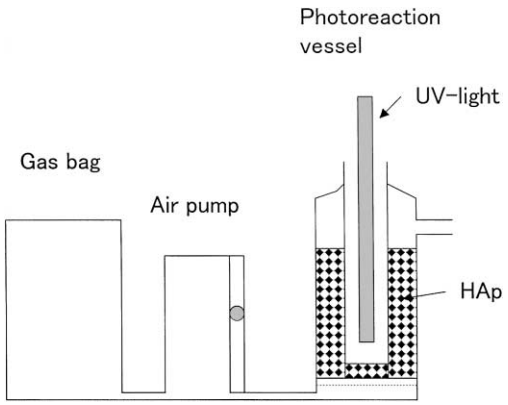

Fig. 1. Schematic diagram of the experimental apparatus.

3. Results and discussion

3.1. XRD and FTIR characteristics

The XRD patterns of the products by an aqueous precipitation procedure followed by heat treatment at 200 and 1150 °C are shown in Fig. 2. All the peaks of the XRD patterns were assigned to those of HAp [17]. The crystallinity of HAp after treatment at 200 °C (HAp200) was lower than that of HAp after treatment at 1150 °C (HAp1150).

The FTIR spectra of the solids are shown in Fig. 3. The peaks around 3400 and 1650 cm^{-1} due to H_2O disappeared in the spectra of HAp1150, though the peaks appeared in those of HAp200. It showed that the structured water left from apatitic structure at 1150 °C. On the other hand, from the result of TG–DTA measurement as shown in Fig. 4, it was recognized that surface-adsorbed water on HAp would desorb below about 200 °C as mentioned in the report of Okada et al. [18]. The desorption above 200 °C is assumed to be that of structural water.

3.2. ESR study before and after UV irradiation

The ESR spectra of HAp200 before and after UV irradiation are shown in Fig. 5. The large peaks at both ends are due to internal standard (MnO). When DMPO was added to the samples, superoxide anion radical $O_2^{\bullet -}$ were detected as DMPO–O_2^- [16]. The characteristic peaks after UV irradiation would show the formation of the DMPO adduct of O_2^-. The small peaks on both sides seems to be DMPO–$CH_3^{\bullet}$. That is, it was recognized that $O_2^{\bullet -}$ species was produced on HAp200 by UV irradiation. The radical is very active for the oxidation of many compounds. The photofunctional effects of HAp200, e.g. photocatalytic

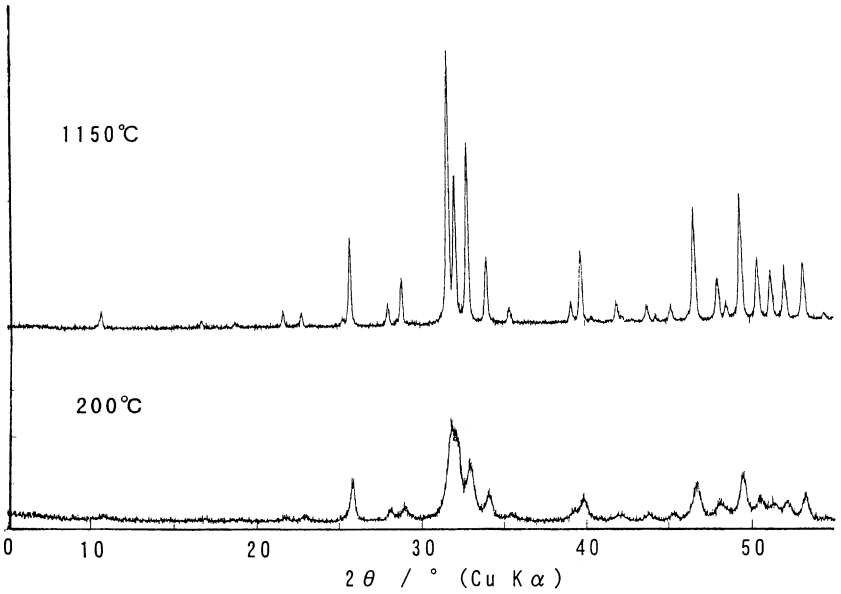

Fig. 2. X-ray diffraction patterns of HAp samples after heat treatment.

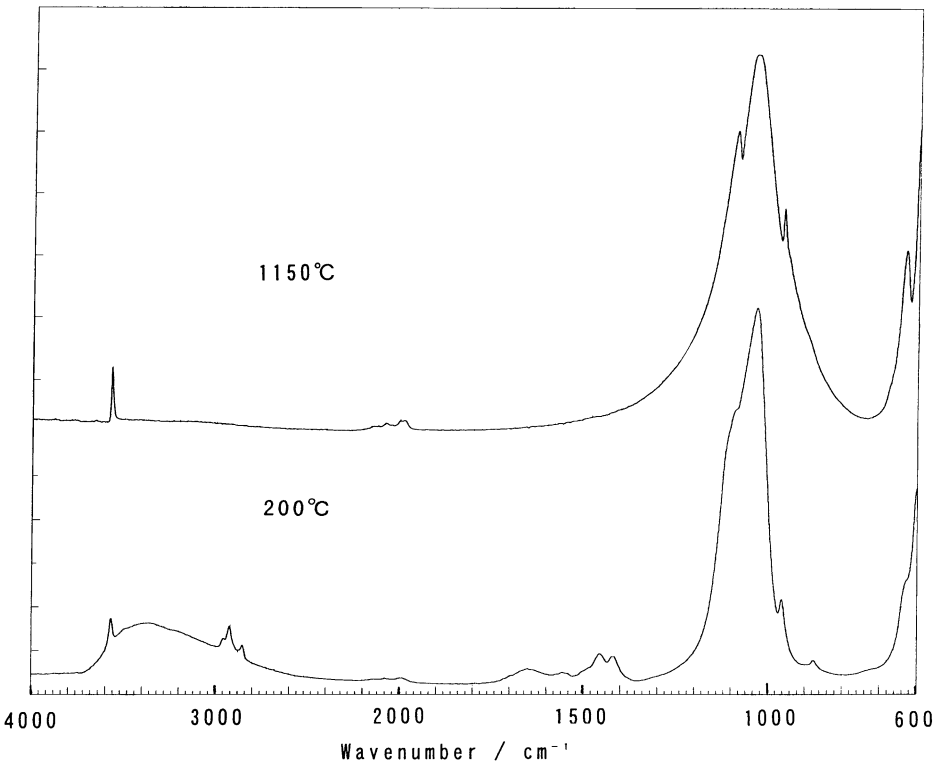

Fig. 3. FTIR spectra of HAp samples after heat treatment.

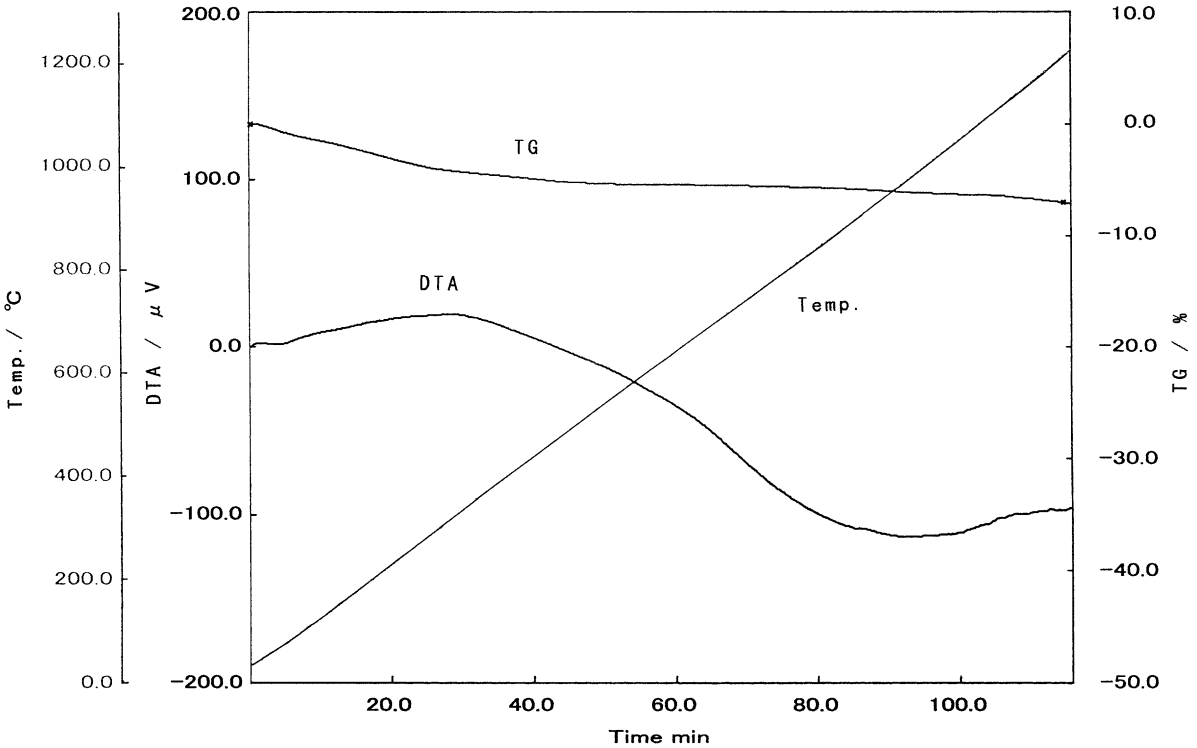

Fig. 4. TG/DTA curves of HAp sample.

decomposition of MM over HAp as described in details later, was assumed to be due to the formation of $O_2^{\bullet -}$ on HAp by UV irradiation. Electron transfer must occur from vacancies on which electron was trapped, formed in apatitic structure to oxygen in atmospheric air on HAp. Therefore, the formation of $O_2^{\bullet -}$ would occur. These phenomena are similar to the behavior of TiO_2, a typical photocatalyst [19,20]. The relationship between UV irradiation time and the signal intensity of DMPO–O_2^- is shown in Fig. 6. The signal intensities became stronger with the increase of irradiation time. It shows that the amounts of $O_2^{\bullet -}$ on HAp200 increase by UV irradiation. These results were different from the result of Kanai et al. [12,13] that active species on HAp were labile O^- species which are generated from OH splitting by light irradiation and that oxygen was treated with O^- to give O_3^-. In our studies, it was assumed that the active and unstable $O_2^{\bullet -}$ species would be generated on HAp200 in connection with the formation of vacancy by UV irradiation. The ESR signal pattern after UV irradiation could support this conclusion [16].

3.3. Adsorption of MM

BET surface area of HAp200 and HAp1150 was 66.5 and 0.025 $m^2\,g^{-1}$, respectively. The reason for the difference between the specific surface area of HAp200 and that of HAp1150 is assumed to be due to the difference of crystallinity. Desorption efficiencies of HAp samples for MM was compared as shown in Fig. 7. The breakthrough of MM occurred after 90 min with HAp200, though it occurred immediately with HAp1150. It was assumed that the difference between the two HAp samples was due to the difference of those specific surface area.

3.4. Photocatalytic decomposition of MM

The comparison of photocatalytic decomposition efficiencies under UV irradiation between HAp200

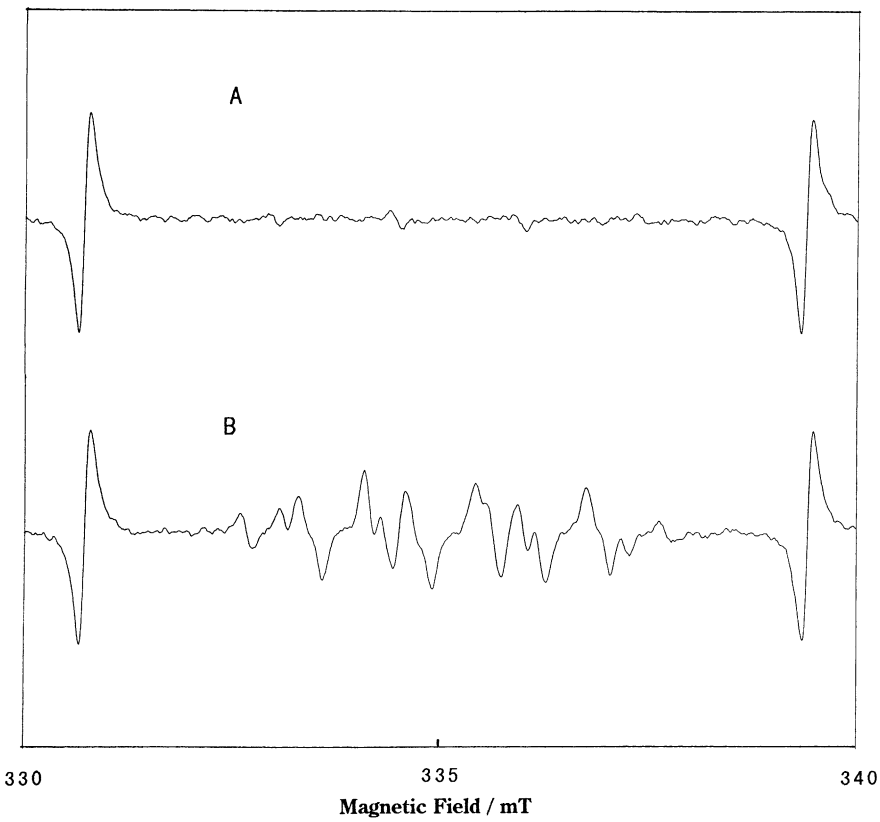

Fig. 5. ESR spectra of HAp200 before and after UV irradiation (DMPO spin adduct): (A) before UV irradiation; (B) after UV irradiation for 60 min.

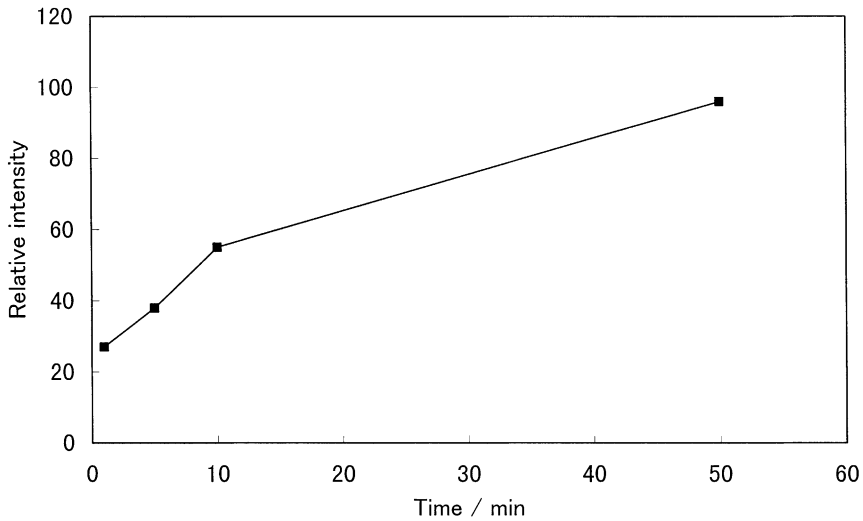

Fig. 6. Effect of irradiation time for ESR signal.

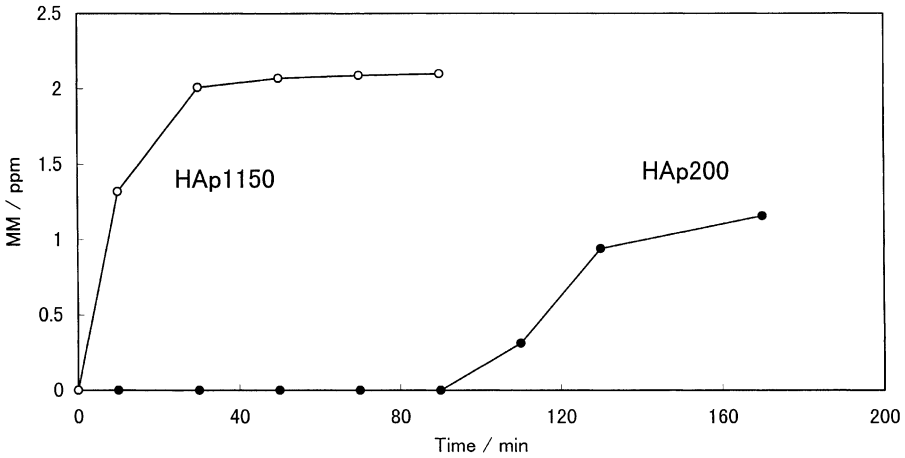

Fig. 7. Desorption curves of MM.

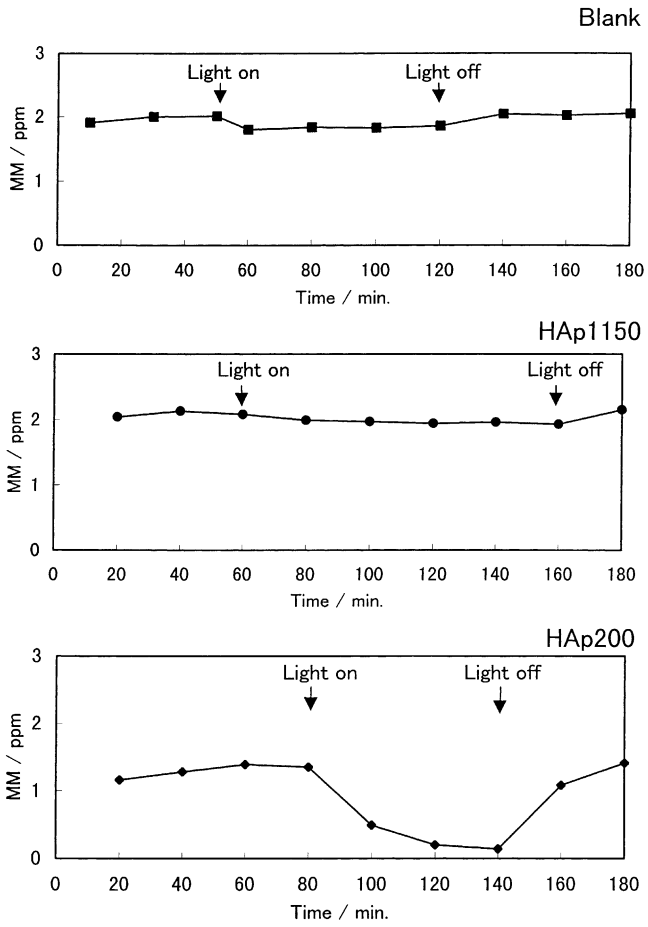

Fig. 8. Comparison of photocatalytic decomposition of MM using two types of HAp.

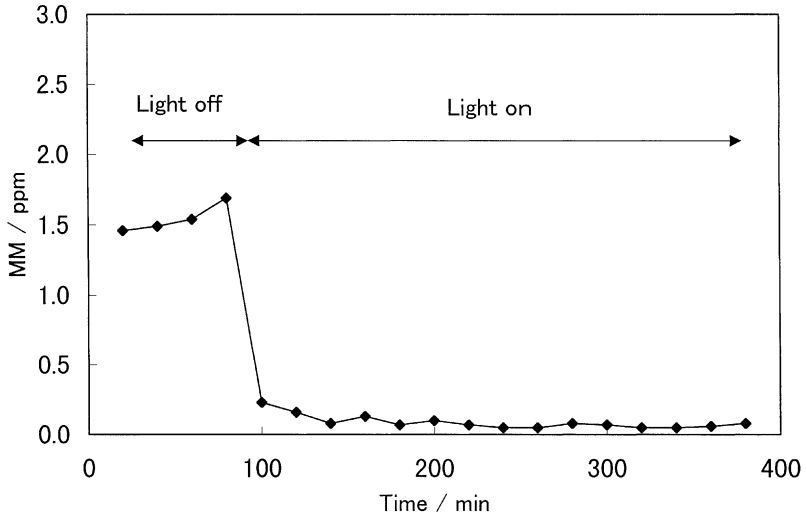

Fig. 9. Continuous photocatalytic decomposition of low concentrations of MM.

and HAp1150 after adsorption/desorption equilibrium of low concentrations of MM is shown in Fig. 8. Photocatalytic decomposition of MM using HAp1150 scarcely occurred as well as blank test. On the other hand, the decomposition of MM using HAp200 was very effective. After UV irradiation for 60 min, the conversion of MM using HAp200 was 96%. The results show that active radical species, that is $O_2^{\bullet -}$ as described above, must produce on the surface of HAp200 by UV irradiation, though the active species seem to scarcely produce on the surface of HAp1150. It is assumed that the difference of the adsorption effect between HAp200 and HAp1150 do not contribute to the photocatalytic decomposition because the decrease of MM on HAp200 occurred by UV irradiation. The photocatalytic decomposition of MM using HAp200 corresponds to the increase of the amounts of $O_2^{\bullet -}$ species as shown in Fig. 6. On the other hand, the conversion of MM using HAp200 under black-light irradiation was about 30%. It shows that the strong energy UV irradiation, that is short wavelength of UV, is necessary for active radical formation on the surface of HAp.

The continuous photocatalytic decomposition of low levels of MM under UV irradiation is shown in Fig. 9. The conversion of MM remained almost constant and effective. DMDS and SO_2, which were oxidative products of MM, were not detected in outlet gas.

3.5. Reaction mechanism for MM

To investigate the decomposition reaction, high concentrations of MM gas (169 ppm, v/v) was used for photocatalytic decomposition under UV irradiation (Fig. 10). The conversion of MM was 35–39% and small amounts of DMDS were determined in outlet gas under UV irradiation. SO_2 and formic acid detected in outlet gas were about 3 and 0.6 ppm (v/v), respectively.

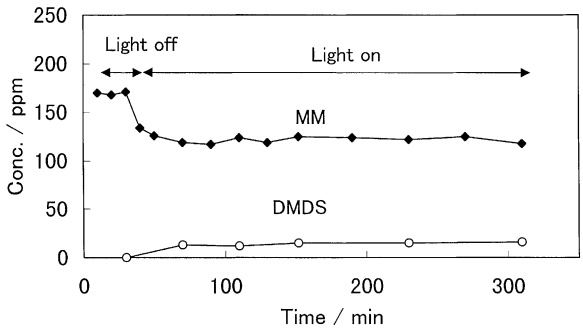

Fig. 10. Continuous photocatalytic decomposition of high concentrations of MM.

Therefore, the photocatalytic reaction for MM over HAp200 would proceed oxidatively as follows:

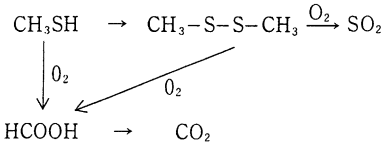

It was recognized that major parts of SO_2 and formic acid produced by the reaction were adsorbed by HAp200 from the results of adsorption test using each pure gaseous compound. This fact indicates that the reason why no products detected in outlet gas in the photocatalytic decomposition with low concentrations of MM was adsorption effect by HAp200.

4. Conclusion

It was recognized that superoxide anion radical $O_2^{\bullet -}$ produced on HAp after heat treatment at 200 °C by UV irradiation. The photofunctional behavior of HAp would be due to the formation of $O_2^{\bullet -}$ by UV irradiation. From the results of ESR studies before and after UV irradiation, it was assumed that the $O_2^{\bullet -}$ species would be generated in connection with the formation of vacancies on the surface of HAp. The photocatalytic decomposition of MM using HAp200 under UV irradiation was very effective, though that using HAp1150 occurred scarcely.

Acknowledgements

The authors thank Dr. K. Tajima, Kyoto Institute of Technology, for his instructive advice. This work was supported by the Koshiyama Research Grant.

References

[1] J.A.S. Bett, L.G. Christner, W.K. Hall, J. Am. Chem. Soc. 89 (1967) 5535.
[2] H. Monma, J. Catal. 75 (1982) 200.
[3] Y. Izumi, S. Sato, K. Urabe, Chem. Lett. (1983) 1649.
[4] W.T. Reichle, J. Catal. 17 (1970) 297.
[5] N.S. Figoli, H.R. Keselman, P.C. Largentiere, C.L. Lazzaroni, J. Catal. 77 (1982) 64.
[6] N.S. Figoli, C.L. Lazzaroni, H.R. Keselman, P.C. Largentiere, J. Catal. 85 (1984) 538.
[7] H. Nishikawa, H. Monma, Nippon Kagaku Kaishi (1991) 1562.
[8] H. Nishikawa, S. Ikeda, H. Monma, Bull. Chem. Soc. Jpn. 66 (1993) 2570.
[9] H. Nishikawa, H. Monma, Phos. Res. Bull. 3 (1993) 115.
[10] H. Nishikawa, H. Monma, Bull. Chem. Soc. Jpn. 67 (1994) 2454.
[11] Y. Matsumura, H. Kanai, J.B. Moffat, J. Chem. Soc., Faraday Trans. 93 (1997) 4383.
[12] H. Kanai, Y. Matsumura, J.B. Moffat, Phos. Res. Bull. 6 (1996) 293.
[13] H. Kanai, Y. Matsumura, J.B. Moffat, Shokubai 39 (1997) 406.
[14] H. Nishikawa, Mater. Lett., in press.
[15] Y. Suwa, H. Banno, M. Mizuno, H. Saito, J. Ceram. Soc. Jpn. 101 (1993) 659.
[16] T. Sekine, T. Masumizu, Y. Maitani, T. Nagai, Int. J. Pharmaceutics 174 (1998) 133.
[17] H. Monma, S. Ueno, M. Tsutsumi, T. Kanazawa, Yogyo Kyokai-Shi 86 (1978) 28.
[18] F. Okada, S. Yuizumi, H. Sakane, T. Hatsushika, T. Suzuki, J. Soc. Inorg. Mater. Jpn. 7 (2000) 185.
[19] R.I. Bickley, F.S. Stone, J. Catal. 31 (1973) 389.
[20] I. Nakamura, N. Negishi, S. Kutsuna, T. Ihara, S. Sugihara, K. Takeuchi, J. Mol. Catal. A: Chemical 161 (2000) 205.